

Simulation of thermal conductivity and heat transport in solids

C. Oligschleger*

*Institut für Algorithmen und Wissenschaftliches Rechnen, GMD – Forschungszentrum Informationstechnik,
D-53754 St. Augustin, Germany*

J. C. Schön

Institut für Anorganische Chemie und SFB408, Universität Bonn, Gerhard-Domagk-Strasse 1, D-53121 Bonn, Germany

(Received 18 August 1998)

Using molecular dynamics (MD) with classical interaction potentials we present calculations of thermal conductivity and heat transport in crystals and glasses. Inducing shock waves and heat pulses into the systems we study the spreading of energy and temperature over the configurations. Phonon decay is investigated by exciting single modes in the structures and monitoring the time evolution of the amplitude using MD in a microcanonical ensemble. As examples, crystalline and amorphous modifications of Selenium and SiO₂ are considered. [S0163-1829(99)02905-7]

I. INTRODUCTION

Thermal conductivity and heat transport play an important role in the understanding of structural and dynamical differences between amorphous and crystalline substances; however, the underlying mechanisms are not yet fully understood. Since the low-temperature experiments by Zeller and Pohl thermal conductivity and specific heat are known to show a universal and anomalous behavior in glasses.¹ Phenomenological models to explain these outstanding effects have been proposed by Anderson *et al.*² and by Phillips *et al.*³ [tunneling in two-level systems (TLS) model], and an extension to somewhat higher temperatures has been worked out by Karpov *et al.*⁴ in order to take into account contributions caused by anharmonic vibrations and thermally activated hopping processes or relaxations in glasses (soft potential model). However, a fully consistent picture requires the analysis of both equilibrium, steady-state and non-equilibrium aspects of the transport properties of solids.

During the last two decades nonequilibrium molecular dynamics (NEMD) has been applied to study such properties, e.g., heat transport, the evolution of shock waves, and decay of phonons.⁵⁻⁸ Based on these pioneering investigations it becomes possible to study the properties of solids using realistic interaction potentials, enabling us to distinguish between the influence of specific features, e.g., the nature of *chemical* bonding, and a more universal behavior, e.g., a more general *physical* dynamics. Since more than 25 years shock waves have been simulated using NEMD (Refs. 9,10) with the focus on shock wave propagation, on plastic deformation of solids or shock wave-induced melting.¹¹ Very recently large-scale computer simulations have been performed to gain insight into plastic deformations in solids induced by shock waves, where the influence of dislocations and defects on the plastic deformation is investigated using NEMD.¹² In these extensive simulations boundary effects could be excluded.

The estimation of phonon lifetimes and their influence on transport properties is stressed by several authors.^{5,13} Ladd *et al.* have calculated the thermal conductivity for an fcc lattice using both density- and heat-flux correlation functions.⁵ Allen and Feldman have investigated the thermal conductivity

in silicon by deriving and evaluating a formula based on the Kubo and Greenwood-Kubo formalism¹³ representing the heat current operator in terms of eigenmodes determined from the dynamic matrix of the disordered Si structure.

Using MD simulations, Michalski has studied the influence of harmonic and anharmonic contributions to the atomic interaction potential on thermal conductivity and heat transport in two-dimensional (quasicrystalline) structures. Furthermore, he has investigated the influence of delocalized and localized modes, the latter being responsible for strong anharmonic effects in glasses.¹⁴

Our work is concerned with molecular dynamics simulations of thermodynamical steady-state and nonequilibrium transport properties in realistic covalent structures, where the main contributions to the thermal conductivity κ and the propagation of heat pulses and shock waves originate from the vibrational degrees of freedom. Our simulations for κ are similar to those of Michalski,¹⁴ but differ from this work by our use of three-dimensional structures with periodic boundary conditions in all lateral dimensions.

One aim of our simulations is to check whether one can simulate and realistically describe thermodynamical properties with “usual” interatomic potentials and structures in a realistic way, and how reliable such potentials and configurations are in modelling heat transport in solids. Another issue we want to address is the importance and influence of structural differences in glasses and crystals regarding heat transport. Here, the computer experiment mimicking the macroscopic setup used to calculate κ , is complemented by the study of phonon decay and wave propagation in such solids.

In the next section, we briefly describe the systems and interaction potentials which we have used. In Sec. III, we explain the methods in detail. The results and comparison with experiments are presented in Sec. IV, followed by a discussion of the results.

II. EXAMPLE SYSTEMS

As representative covalent materials we have used Se and SiO₂. Selenium readily forms glasses and amorphous

structures.¹⁵ Several crystalline structures exist, including two (α - and β -) monoclinic forms with four eight-membered rings packed differently in the unit cell. Under standard conditions the most stable crystalline phase consists of infinite parallel helical chains with trigonal symmetry.^{15,16} We used this so-called trigonal (t -)Se for our investigations of crystalline selenium.

The potential used to simulate Se has been described earlier.¹⁷ The parametrization of the potential was chosen to mimic certain structural properties of selenium: The potential was fitted to reproduce bond lengths, angles, and bonding energies of small Se molecules,^{18,19} and to give a reasonable description of the trigonal crystal.^{16,20,21}

SiO₂ exists in many different crystalline allotropes (e.g., α and β quartz, high and low cristobalite, tridymite, keatite, coesite, and stishovite)²² and is known to be a strong glass former.^{23–25} The atomic interaction potential was fitted by Vashishta *et al.*²⁶ in order to reproduce structural and dynamical properties of both crystalline and glassy phases.

From experiment it is known that α -SiO₂ has a quite high thermal conductivity compared to others glasses²⁷ which have typically thermal conductivities of the order of several 0.1 W/mK. Using these empirical potentials for Se and SiO₂ glasses are generated by rapid MD quenches from well equilibrated liquids^{28,29} and a final quench to 0 K.

III. METHODS AND CALCULATIONS

With molecular dynamics (MD) one can simulate and investigate properties of complex systems.^{30–34} In order to determine structural, dynamical and thermodynamical quantities one typically explores correlation functions (e.g., van Hove correlation to get insight into the radial distribution of atomic distances, and velocity autocorrelation³⁵ or displacement autocorrelation³⁶ to calculate the vibrational spectrum of configurations). Here we want to describe a more direct way to determine thermal properties of solids.

A. Thermal conductivity

Experimentally the thermal conductivity is determined by measuring the *stationary* heat flux necessary to maintain a temperature gradient generated by two heaters in the sample.³⁷ One fundamental problem in experiment is the thermal insulation of the sample against heat loss to the surroundings. Note that in computer experiments this problem can be avoided by imposing periodic boundary conditions.

In this paper we describe a simulation which is designed to mimic the experimental setup. First we equilibrate configurations (with $N = 1470$ to 23 520 particles) at temperature T for several thousand MD time steps (typically 4000 to 40 000 MDS). In order to determine the thermal conductivity κ of a given structure, we select two ‘‘contact’’ layers of atoms (typically about 10% of all atoms comprising the structure) and fix the average temperatures in these layers at $T_L = T \pm \Delta T$ by scaling the atomic velocities according to the formula $\frac{3}{2}Nk_B T = E_{\text{kin}}$. For symmetry reasons these layers are separated by half the box length. In order to reduce surface effects we apply periodic boundary conditions in all spatial directions. The setup of our computer experiment is sketched in Fig. 1. The atoms outside these layers are al-

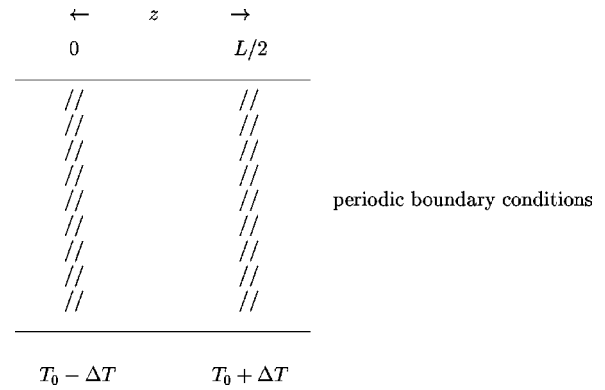


FIG. 1. Realization of the computer experiment in order to determine the thermal conductivity of solids. In all spatial directions we apply periodic boundary conditions. The shaded areas symbolize the layers where the temperatures are fixed.

lowed to move according to Newton’s laws. The velocities of these particles are not rescaled. After some time (typically several thousand MDS) a stationary temperature gradient $2\Delta T/L/2$ has developed. To determine the temperature gradient, we calculate the ‘‘local’’ temperature (i.e., the kinetic energy) of sublayers of the structure by dividing the system into parallel layers of equal thickness in which we measure the ‘‘local’’ (kinetic) temperature as described in Refs. 8,38. In Fig. 2 we plot the temperature of the sublayers versus the z coordinate of the layers ($z \in [-L/2, L/2]$ corresponds to the original box, the additional points are plotted to show the periodic boundary conditions). The fluctuations of the mean temperatures in those subensembles for which we do not regulate the temperature are about $\pm 4\%$, whereas in the two layers, where the temperature is fixed by scaling the velocity, the local temperatures change about $\pm 2\%$ (this is the change of the local temperature in one time step *before* scaling). Note the clear development of a *linear* temperature gradient during the simulation. This shows the development of a steady nonequilibrium state, which enables us to use Fourier’s law of heat flow,^{14,38,39} where the heat flux j necessary to maintain the temperature difference $2\Delta T$ is given by

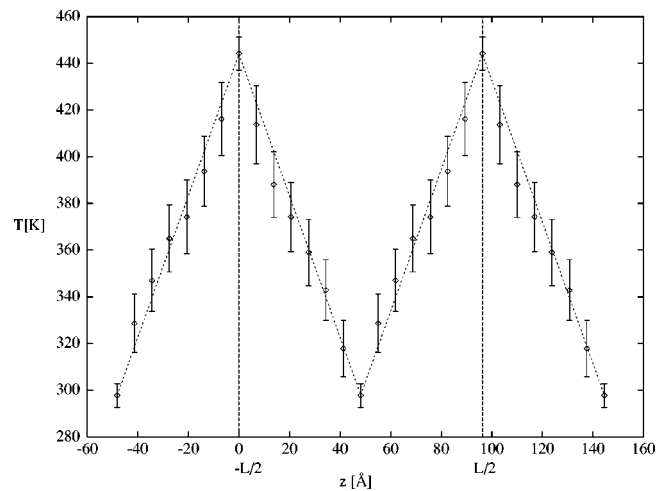


FIG. 2. Mean temperatures in the sublayers of the structure vs the z axis.

$$j = \frac{\langle \Delta E \rangle}{A \Delta t} = -\kappa \frac{2 \Delta T}{(L/2)}. \quad (1)$$

Here, Δt is the time step used in the MD simulation, A is the interface area of the sample perpendicular to the heat flux, and $\langle \Delta E \rangle$ is the average energy per time step Δt which is added and subtracted, respectively, in the layers representing the heat contacts. The changes of the energy $\langle \Delta E \rangle$ are determined by the changes of the temperatures of the layers: We heat and cool the layers by rescaling the velocities of the particles comprising the layers, i.e., changing the atomic velocities from \mathbf{v}_i (before scaling) to \mathbf{v}'_i (after scaling). Therefore, the energy difference is given by $\langle \Delta E \rangle = \langle \Delta E_{\text{kin}} \rangle = \langle \frac{1}{2} \sum_{i=1}^{N_L} m_i (\mathbf{v}'_i{}^2 - \mathbf{v}_i^2) \rangle = \frac{3}{2} N_L k_B \langle \delta T_L \rangle$, with N_L the numbers of atoms in the layers (large enough to define a sensible local temperature) and $\langle \delta T_L \rangle$ the temperature change necessary to maintain the desired temperature $T_L = T \pm \Delta T$ of the layers. The amount $\langle \delta T_L \rangle$ is averaged over the last 20 000 MDS of our simulation. To avoid quantum effects, which we cannot account for (e.g., tunneling in two-level systems), we have chosen “intermediate” temperatures to simulate and to measure thermal conductivity. In order to test our “computer experiment,” we vary (a) the temperature gradients, (b) the layer thicknesses, (c) the temperatures, and (d) the system size.

(a) We find that temperature differences between the contact layers ranging from 20 to 40% of the average temperature are sufficient to reach convergence in the “measurement” of $\langle \Delta E \rangle$ in reasonable computer time. However, in typical computer simulations the temperature gradients are of the order 10^{10} K/m, which is orders of magnitudes higher than in experiments. Such large gradients might have a strong influence on the decay of phonons.

(b) We have varied N_L from 1 to 20 % of the total number of atoms N in the simulation cell. In our experience we get fast convergence of the results by using about $N_L = 0.1 N$ atoms in the layers.

(c) The temperatures used in our simulations range from several K upwards to about 400 K. At temperatures below 1 K, the physical effects in solids are dominated by quantum effects which our classical simulation method cannot describe. On the other hand, very high temperatures lead to large displacements of the atoms in the layers, and the interfaces of the layers and the rest of the system roughen considerably. Simulating Se glass at temperatures ranging from 3.5 to 170 K, we observe mean displacements $\langle u \rangle = 0.6$ to 0.8 \AA per atom. In trigonal Se the mean displacement of the particles is about 0.2 \AA per atom at $T = 370 \text{ K}$.

The drift in the total energy of the configurations is less than 4 parts in 10^4 for the highest temperature employed and less than 3 parts in 10^6 for the lowest temperature simulated. The reason for this energy drift is the use of an isothermal “subensemble” in the part of the system where we fix the temperature, while treating the rest of the system as a microcanonical ensemble where the total energy is conserved.

(d) From experiment one knows that in “perfectly” crystalline but finite structures the thermal conductivity depends on the lateral dimensions of the samples. The smaller the crystalline sample, the smaller is the measured thermal conductivity. In such confined structures the mean free path of

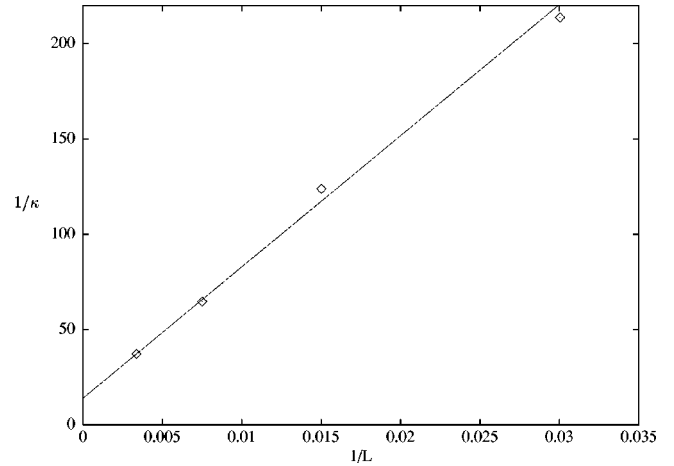


FIG. 3. The inverse thermal conductivity in $[\text{W/cm K}]^{-1}$ for different system sizes plotted versus inverse system size in reduced units at $T = 90 \text{ K}$ for t -Se.

the phonons is limited by the surfaces of the experimental probes which act as scatterers for the phonons. This phenomenon is known as Casimir limit.⁴⁰ In computer simulations where one deals with small (typically nanoscale) structures, the influence of the system size will be even stronger than in experiments with sample diameter of the order of mm. In order to deal with this phenomenon, we have performed simulations for several system sizes L and extrapolated the thermal conductivity for $L \rightarrow \infty$. In Fig. 3 we show the inverse of the thermal conductivity versus the inverse of the layer distance for t -Se.

B. Heat pulse

To study the dissipation and spread of kinetic energy in the system we induce a heat pulse into the system after it has equilibrated. We scale the atomic velocities in a layer with N_L particles (typically 15% of the sample) to be much higher than the averaged velocities of the atoms outside this layer. After this initial heat pulse the sample is allowed to evolve freely. Again we calculate the “local” temperatures for a sequence of sublayers.³⁸

The time evolution of the local temperature $T(t)$ in the different layers provides insights into the mechanisms underlying the energy transfer in the system.⁸ In particular comparing the evolution of crystalline and glassy systems elucidates differences in heat transport caused by the structure of the samples. Especially the Fourier transform of $T(t)$ can be used to identify modes and vibrations responsible for heat transport. We have applied heat pulses to amorphous Se and trigonal Se, both parallel and perpendicular to the helical chains.

C. Shock waves

The sound velocities of the structures can be determined from the effects of moderate shock waves in the system.¹⁴ We generate such a wave by shifting the atoms of one layer ($N_L = 0.02 - 0.05 N$) from their equilibrium positions by about 2.5% of the nearest-neighbor distance in one direction and follow the development of the perturbation. As initial condition the atomic velocities are set to zero. Measuring the

“local” (kinetic) temperatures (as in Ref. 38) in the sublayers at every time step we derive the sound velocity from the space-time evolution of the temperature. We have applied this procedure to trigonal Se both parallel and perpendicular to the chains, to α quartz, and to amorphous Selenium and SiO_2 .

D. Decay of modes

One of the central questions in the field of heat transport concerns the lifetime of phonons. In perfectly harmonic crystals, the lifetime of phonons would be infinite. However, due to anharmonic contributions to the potential, which gain importance with increasing temperature, the mean free path of the phonons is limited by umklapp processes. On the other hand, at very low temperatures, when the umklapp processes are effectively frozen out, the only limiting factors of thermal conductivity and of lifetimes and mean free paths of phonons are the scattering of phonons due to surface effects (Casimir limit) and/or impurities or defects of the structures. In real materials the thermal conductivity is also limited by electron-phonon interactions and isotope effects.^{41,42} Clearly, the description of processes in terms of phonons depends strongly on whether the exact states in anharmonic systems can be approximated by phonons, i.e., whether the phonons decay slowly enough to allow a meaningful description of the instantaneous state of the system in terms of vibrational modes.

The phonons, which correspond to the eigenvectors (EV's) of the dynamical matrix of the system, are determined in harmonic approximation by diagonalization of this matrix.⁴³ Since the number of eigenvectors ($3N$, N being the number of particles in the simulation cell) is very large, we can only estimate the lifetimes for a subset of the EV's. In order to determine the lifetime of a phonon, we excite an eigenmode \vec{e}_j (normalized to unity) in the system by displacing the atoms according to their contributions to the corresponding eigenvector, and follow the time evolution of the atomic motion using NVE-MD where the number of atoms, the volume and the total energy are kept constant. The original displacement is given by

$$\Delta\vec{r}(0) = \alpha\vec{e}_j, \quad (2)$$

where α is the amplitude of the displacement vector.

During the MD simulation we calculate the projection of the actual atomic displacement onto a subspace of eigenmodes $\{\vec{e}_m\}$:

$$c_{re_m} = \frac{\Delta\vec{r}(t) \cdot \vec{e}_m}{|\Delta\vec{r}(t)|}. \quad (3)$$

The projection on the eigenmode \vec{e}_j will have the period $\tau_j = 1/\nu_j$ of the excited eigenmode, and the amplitude will be constant as long as no interactions with other modes occur, i.e., as long as the mode does not decay. Due to the anharmonic interactions between the eigenvectors other modes will become excited. The calculation of the expansion coefficients $c_{re_m}^2$ (with $m \neq j$) allows to monitor the excitation of other modes \vec{e}_m . With this procedure one can follow the time evolution of *single* phonons or modes of the solids. The

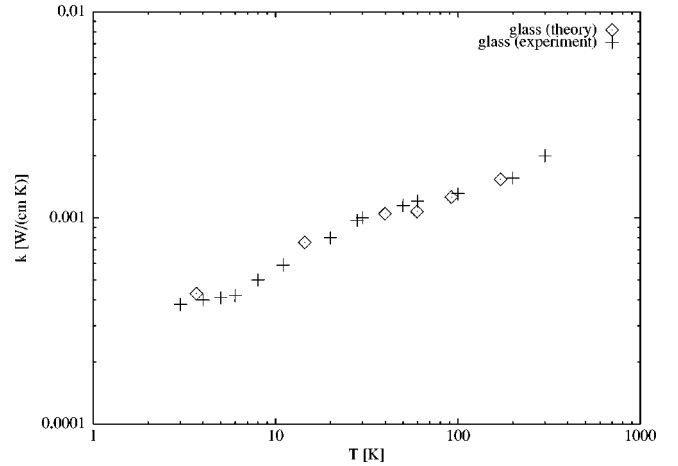


FIG. 4. Thermal conductivity κ [W/cm K] of Se glass plotted versus temperature T in K in a double logarithmic plot. \diamond : simulation, $+$: experimental values from Ref. 46.

usual dynamic structure factor $S(\vec{Q}, \nu)$ can be used to obtain information on the broadening of peaks and frequency shifts of typically *groups of modes*, but only little knowledge about the types of modes involved and their detailed interactions. The development of single modes can be extracted in the one-phonon approximation.^{7,44} Using the projection procedure, we have investigated the *t*-Se crystal and Se glasses.

IV. RESULTS

A. Thermal conductivity

Using the algorithms described in Sec. III A we have simulated the thermal heat conduction κ_{\parallel} (parallel to the chains) of trigonal Se. The limitations of the very short distance L between the layers kept at fixed temperatures $T_L = T \pm \Delta T$, which is computationally accessible, suggest an extrapolation of the distance to infinity. The simulation at $T = 25$ K yields $\kappa = 0.033$ W/(cm K) for $N = 23\,520$ atoms. Extrapolating $L \rightarrow \infty$ gives $\kappa(L = \infty) = 0.072$ W/(cm K), which is about a factor of 6 lower than the experimental result.⁴⁵ At $T = 90$ K even the largest simulated system with $N = 23\,520$ atoms deviates from the experimental value by more than a factor 3.8. In the limit of infinite system size, we find $\kappa(L = \infty) = 0.071$ W/(cm K) for trigonal Se. This result is 30% lower than the experimental result. At $T = 370$ K we extrapolate $\kappa(L = \infty) = 0.017$ W/(cm K) which deviates from the experimental value $\kappa = 0.0538$ W/(cm K) measured at $T = 400$ K.⁴⁵ At temperatures above $T = 350$ K photons contribute to the thermal conductivity which lead to an increase of κ .²⁷ The discrepancies may be due to some short-comings of the potential which we use to model Se, especially the low-frequency phonons are described insufficiently.¹⁷

In the case of Se glasses, we find a much better agreement between the results of our simulations and the experimental findings. In Fig. 4 we plot the thermal conductivity versus temperature with double-logarithmic scales. In the whole temperature range covered, the deviation between the theoretical values and the experimental ones⁴⁶ never exceeds 20–30%. Furthermore, no significant system size effect has been detected in our calculations.

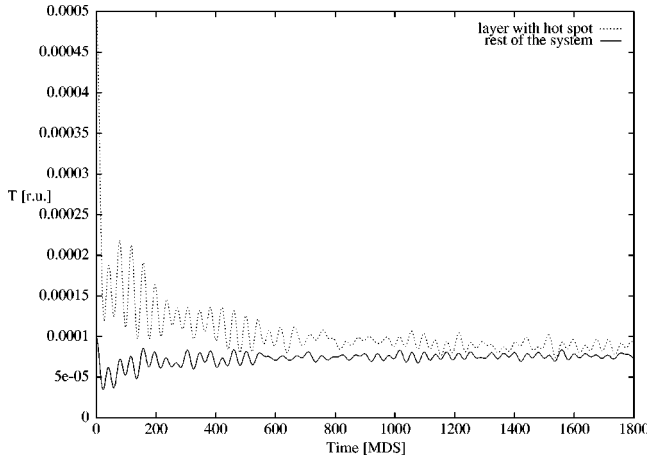


FIG. 5. Evolution of the local temperature of the layer $T_l(t)$ (dotted line) and the rest of the crystal $T_r(t)$ (solid line) in K vs time in MDS after a hot spot was induced into a layer parallel to the chains a trigonal Selenium crystallite with $N=1470$ atoms. The typical period of temperature changes is about 77 fs.

Our simulations of SiO_2 glasses show a different behavior, however. To gain results of thermal conductivities comparable with experiment it was necessary to construct glasses with L up to 125 Å. From these we were able to extrapolate the thermal conductivity in the limit $L \rightarrow \infty$ as upper bound of the computed thermal conductivity in SiO_2 glasses. At $T = 60$ K we find $\kappa = 0.59$ W/(mK), a result 25% higher than the experimental value.⁴⁷ Here one should note that the phonon spectrum calculated using the potential for SiO_2 given in Sec. II overestimates the low-frequency modes,²⁶ while the calculated spectrum for Se underestimates the low-frequency phonons.¹⁷

B. Heat pulse

In a trigonal Se crystal consisting of 1470 atoms we excited in one layer parallel to the z axis a heat pulse with a local temperature which was 5 times higher than the temperature in the rest of the system. The layer comprised 210 atoms (14 chains with 15 atoms). We observed the spread of the energy in the system. By symmetry the direction of the flow was perpendicular to the chains of the crystal. The evolution of the “local” temperature (i.e., the kinetic energy) of the layer $T_l(t)$ and of the rest of the system $T_r(t)$ are shown in Fig. 5 as dotted and solid lines, respectively. From Fig. 5 one can deduce that the velocities of the atoms in the layer with the induced higher temperature change with a period of about 0.15 ps (corresponding to a frequency of 6.5 THz) and additional lower-frequency modulations in the case of crystalline trigonal Se.

The Fourier transforms of $T_{l,r}(t)$ are shown in Fig. 6. Since $T \propto v^2$ the frequencies of the temperature changes are a factor of 2 higher than the corresponding changes of the velocities. However, taking this factor 2 into account the power spectrum resulting from the Fourier transform of $T_r(t)$ resembles in some features the usual density of states DOS.^{17,48} On the other hand, the power spectrum associated with the temperature evolution of the excited layer shows strong contributions at low frequencies (caused by the strong exponential decay of the temperature of this layer: the “re-

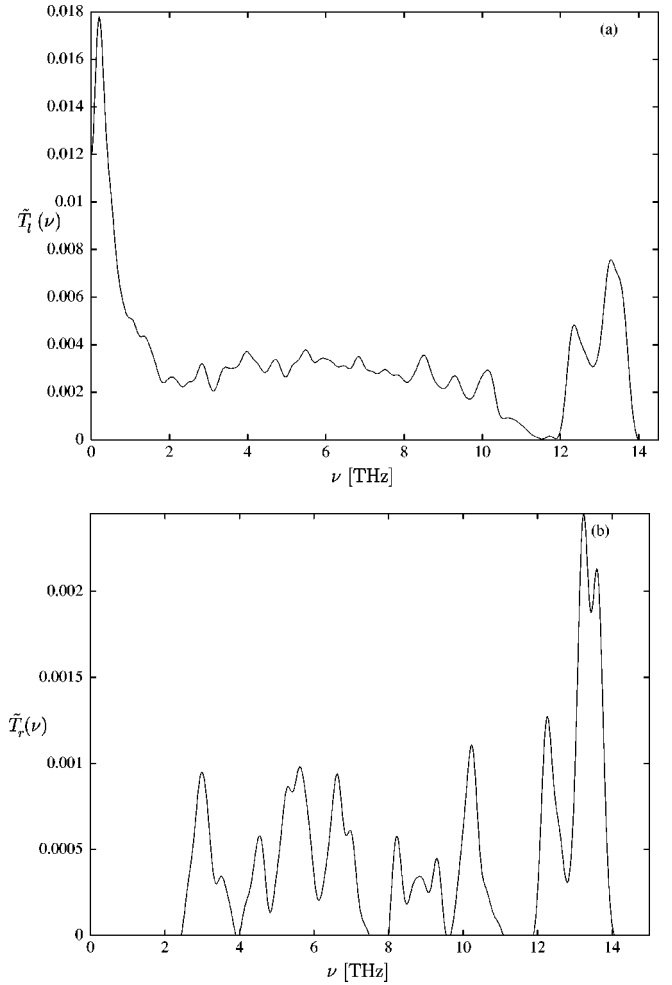


FIG. 6. Fourier transform (power spectrum) $\tilde{T}_l(\nu)$ (a) and $\tilde{T}_r(\nu)$ (b) of $T_{l,r}(t)$ of Fig. 5.

laxation time” is about 350 MDS ≈ 0.7 ps). These modes reflect the “dissipative” character of the evolution of the (kinetic) temperature in the layer exposed to the heat pulse. Apart from this dominating peak due to the fast decrease in temperature at the beginning of the MD run, we find familiar contributions at the high frequency end caused by bond stretching modes, and a broad spectrum towards lower frequencies.^{17,49}

In another simulation, we excited a heat pulse in a layer parallel to the basal plane of t -Se. Again, the energy dissipation of the excited layer causes a strong peak to appear at the low-frequency part of the spectrum. However, we again find bond stretching modes clearly developed in the power spectrum. The high frequency part of the spectrum of excited vibrations in $\tilde{T}_r(\nu)$ resembles the one we calculate in the case of perpendicular heat flow, but some deviations in the middle of the spectrum occur. This part of the spectrum is assigned to librations and bond-bending vibrations.¹⁷

We have performed the same simulations for a Se glass consisting of 1470 atoms. We observed a fast (exponential) “heat relaxation” of the induced thermal energy, as in the case of t -Se. Again, the power spectrum $\tilde{T}_r(\nu)$ exhibit some similarities with the typical vibrational DOS of a -Se.

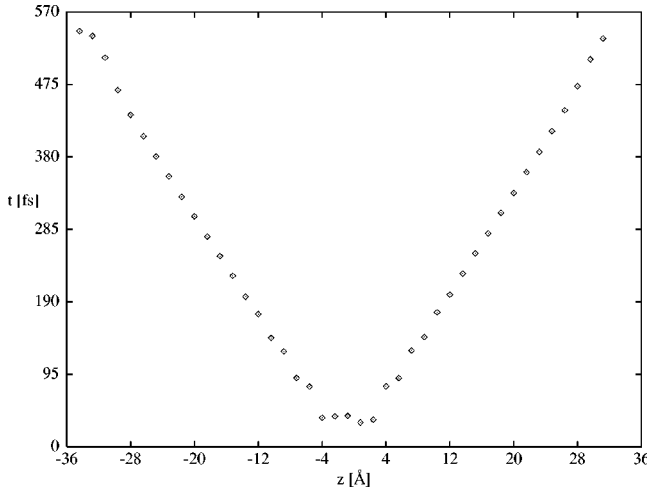


FIG. 7. Times in fs needed for the perturbation to reach the layers are plotted vs the distance of the layers in Å along the direction of propagation.

C. Shock waves

We have determined the sound velocities of solids from the analysis of shock waves both for crystals and glasses (*t*-Se, α -quartz, *a*-Se, and *a*-SiO₂). We divided the trigonal Se crystal with $N=2940$ atoms into 42 layers perpendicular to the chains and studied the time evolution of a perturbation induced in the system by displacing the atoms of one layer of the structure from their equilibrium positions by about 0.05 Å in the z direction. As described in Sec. III C, we monitor the development of the local temperature of the layers. The sound velocity of the system can be derived by plotting the time necessary for the perturbation to reach the various layers along the system. In Fig. 7 the times are plotted versus the layers along the z axis, yielding a sound velocity $v_z=5690$ m/s. This result agrees well with earlier results obtained for the longitudinal sound velocity $c_{33}=5630$ m/s.¹⁷

After dividing the trigonal Se in layers oriented parallel to the chains (and perpendicular to the x axis) and displacing the atoms of one layer in the x direction, we again measured the speed of the heat pulse, finding an effective sound velocity in the x direction $v_x=4600$ m/s. Due to the symmetry of the trigonal structure, this result is by a factor of $\cos 30^\circ$ smaller than the longitudinal sound velocity $v_{11}=5330$ m/s calculated previously.¹⁷

To calculate the sound velocity of α quartz, we investigated the time evolution of a perturbation induced in the system by displacing the atoms of the central layer from their equilibrium positions by about 0.02 Å in the z direction. The structure comprising $N=2356$ atoms was divided into 24 layers perpendicular to the z direction. Following the same procedure as before, we calculated the sound velocity $v_z=8335$ m/s. This result agrees well with the longitudinal sound velocity $c_{33}=8250$ m/s obtained from the elastic constant $C_{33}\approx 180$ GPa.⁵⁰

Next we investigated both *a*-Se with $N=1470$ particles and *a*-SiO₂ with $N=3456$ atoms. We divided the structures into 21 and 24 parallel layers, respectively. These layers were oriented perpendicular to the z axis, and we induced a perturbation into the glasses by displacing all the atoms in

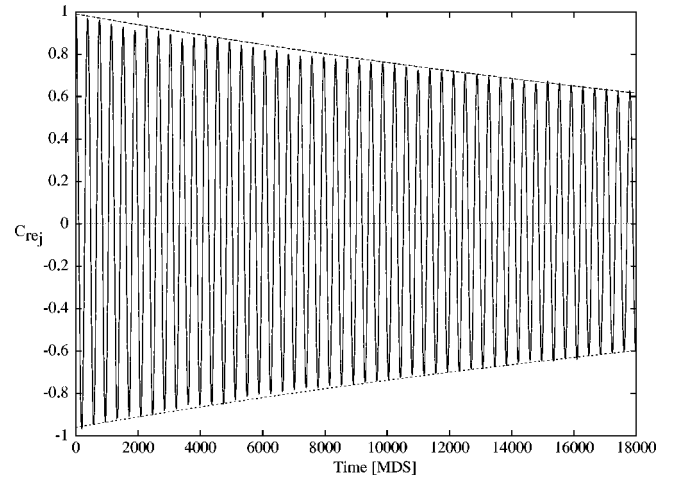


FIG. 8. Projection c_{rej} of the actual displacement onto the initially activated eigenvector for a mode with $\nu=1.36$ THz in the *t*-Se vs time in MDS. The system is equilibrated at $T=60$ K. The envelopes of the projections are two exponential functions.

the middle of the system in the positive z direction by about 0.05 and 0.02 Å, respectively. As before, we observed the time dependence of the induced shock wave by following the kinetic temperature evolution of the various layers. In both cases we did not observe any clearcut wavelike perturbation propagating through the system. Therefore, it was impossible to determine reliably, or at least to estimate the sound velocities of the glasses from these simulations. This negative outcome of the analysis of the behavior of shock waves in glassy and disordered structures contrasts with the findings for the crystalline counterparts and might be traced back to structural differences, e.g., the lack of long-range order in amorphous structures. Thus structural defects in glasses might cause the ‘‘overdamping’’ of the wave, which is most likely related to the rather fast decay of phonons in glasses (see Sec. IV D).

D. Decay of modes

Exciting single modes in the system allows us to study their time evolution. We applied the procedure described in Sec. III D to a subset of modes only, since the trigonal Se-crystallite chosen comprised $N=1470$ atoms. In the low-frequency regime ($\nu\leq 5$ THz) we investigated the decay of $n(=25)$ modes. To estimate the influence of temperature, we excited the EV’s both for the $T=0$ K configuration and for a crystalline configuration equilibrated at $T=60$ K. In Fig. 8 we plot the projection c_{rej} [see Eq. (5)] versus observation time t . The initially excited mode has a frequency $\nu=1.39$ THz and is delocalized, its participation ratio being $p_\nu=0.62$. The envelope of the projection exhibits an exponential decay with a time constant $\tau\approx 70$ ps. The Fourier transform gives insight into the frequency shift of the modes due to anharmonic effects and into the spectral broadening of the mode. The latter effect is also relevant for the lifetime of a mode but not so reliable due to the finite simulation time. The Fourier transform of the projection c_{rej} shown in Fig. 8 leads to the spectral density plotted in Fig. 9 with a maximum at $\nu=1.36$ THz. This shift in frequency means that the

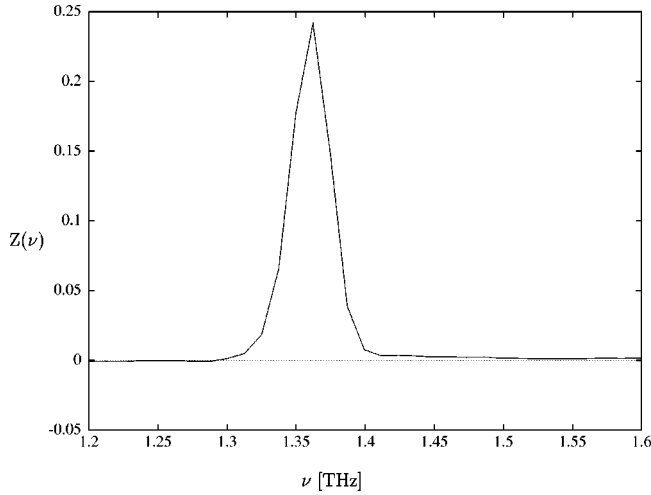


FIG. 9. Fourier transform of the projection c_{re_j} shown in Fig. 8.

mode has softened with temperature.⁴² In order to verify, whether the shift in frequency is due to temperature effects or is an artifact of the damping of the mode, we have calculated the Fourier transform of $\cos(\omega t)\exp(-t/\tau)$ with $\omega = 1.39$ THz and with $\tau \approx 7 \times 10^{-10}, 7 \times 10^{-11}, 7 \times 10^{-12}$ s. Even for the shortest decay time τ we find a shift less than $10^{-4}\omega$. Thus we conclude that the observed shift in frequency is really caused by the influence of the temperature on the modes, in qualitative agreement with the softening observed in experiment.⁴²

Due to interactions between the modes additional frequencies are excited in the system. In order to estimate the excitation of additional modes, we have calculated the projections of the actual displacement on modes $\{\vec{e}_m\}$ with frequencies similar to the initially excited one. We sum the square of the projections on 50 modes. After an observation time of about 35 ps, the square of the expansion coefficient of the initially excited mode is still larger than 0.6, and the sum for the energetically similar modes is 0.3. Obviously, the atomic displacements are still restricted to a small subspace of EV's. Thus, only 1% of the eigenmodes of the configuration are needed to describe the atomic motions to more than 90%.

This detailed analysis can be complemented by a calculation of $S(\vec{Q}, \nu)$ that has the advantage to be directly comparable with experiment. However, in general for a given \vec{Q} several phonons contribute to the same $S(\vec{Q}, \nu)$. Therefore, an unambiguous assignment of the spectrum of $S(\vec{Q}, \nu)$ to single modes is not possible. As an example we show in Fig. 10 for two values of \vec{Q} in the $[0 \ \xi \ 0]$ direction the resulting $S(\vec{Q}, \nu)$. The estimate of the lifetime by full width at half maximum (FWHM) yield for the dominant phonon in $\vec{Q} = 2\pi/a[0 \ 0.2 \ 0]$ approximately 25 ps. But due to the superposition of the peaks it is difficult to estimate the lifetimes of the other phonons. In particular, there are several phonons which cannot be investigated calculating only $S(\vec{Q}, \nu)$ because of this \vec{Q} selectivity.

In the high-frequency regime we followed the time evolution of a mode just above the gap of the DOS. The eigenfrequency of this (localized) mode was $\nu = 6.2$ THz, and it decayed within 2 ps. However, the simulations of extended

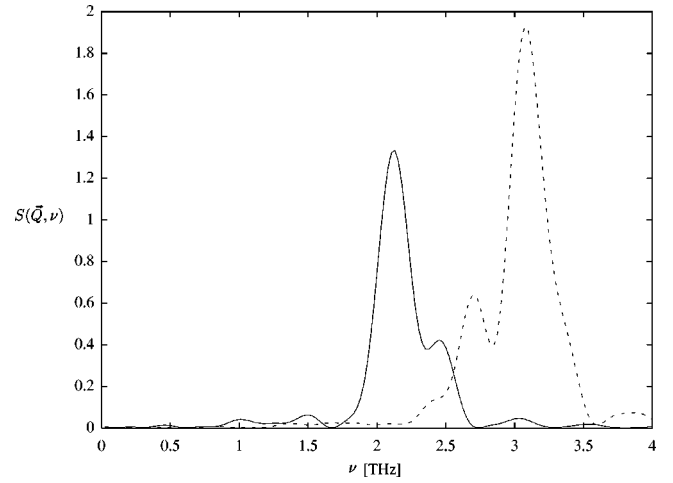


FIG. 10. Structure factor $S(\vec{Q}, \nu)$ in the $[0 \ \xi \ 0]$ direction for two values of \vec{Q} : solid line $\vec{Q} = 2\pi/a[0 \ 0.2 \ 0]$ and dashed line $\vec{Q} = 2\pi/a[0 \ 0.3 \ 0]$.

modes in the high frequency end of the DOS did not show any appreciable decay of the EV's within the observation time.

For glasses, the behavior of the modes is totally different. We have diagonalized the dynamical matrix of one Se glass and calculated the EV's. In the low-frequency regime there exist beside extended eigenvectors a few quasilocalized modes, while in the high-frequency part of the spectrum nearly all modes are localized. In the regimes of low, medium, and high frequencies we have performed similar simulations as in the case of trigonal Se. For a quasilocalized mode (with a frequency $\nu = 0.31$ THz and a participation ratio $p_\nu = 0.09$) we observe a fast decay of the eigenmode. No clear vibration develops or can be identified in the glass. During the MD run, we also checked, whether a subset of about 20 modes with similar frequencies might be more stable. When analyzing phonons in the low-frequency regime we found that this small subset of eigenmodes (less than 1% of the EV of the configuration) described the atomic motions to an extent of about 30%. The phonons of the medium and high-frequency regime were much less stable and decayed within several ps.

Finally we considered the decay of phonons in the non-equilibrium steady state, in order to estimate the influence of the strong temperature gradient on the lifetimes of the eigenvectors. We excited some phonons in a *t*-Se crystallite with $N = 1470$ atoms, where two layers were kept at fixed temperatures $T_L = T \pm \Delta T$, and monitored the projection of the actual displacement onto the additionally excited eigenvector. In comparison with the lifetime of the same mode excited in a configuration with constant temperature, the phonon proved to be much less stable: typically about a factor of 5. However, since we extrapolate to infinite system size keeping the temperature difference between the contacts constant, the effect of the strong temperature gradient present during the simulations should be largely eliminated when calculating $\kappa(L = \infty)$.

V. SUMMARY AND CONCLUSION

In this paper we have presented simulations of steady-state and nonequilibrium thermal heat transport in condensed

matter. As examples we used Selenium and SiO_2 , both in crystalline and amorphous modifications.

In the crystalline structures the thermal conductivity showed a clear system size dependence (Casimir limit), due to the restrictions of the mean free path of the phonons by the lateral dimension of the simulation cell. Extrapolation of the system size L to infinity yielded values of the thermal conductivity of the same order of magnitude as the experimental results. Since there are no impurities in the system, the phonons are not scattered at structural defects, vice versa this means that the lifetimes of the eigenmodes are limited only by anharmonic effects of the atomic interaction potential.

In glasses the situation is rather different. In the case of Selenium glasses, it was sufficient to simulate structures comprising 1470 particles in the simulation cell to reach convergence of the results for the thermal conductivity. This can be understood considering that the amorphous structure, or to be more precise the state of disorder itself, is the reason for the anomalous and universal behavior of thermal heat transport in glasses. The phonons decay fast within several ps. But nevertheless, the eigenmodes typically interact with energetically similar modes⁵¹ which means that the "subspace" of modes is relatively stable. Quartz glass is known to possess extremely large mean free paths of phonons;²⁷ this agrees with our observation that it was necessary to construct glass configurations with $L \approx 125 \text{ \AA}$ in order to get results comparable to the experimental findings.

It is a striking result of our work that the agreement between theory and experiment for thermal conductivity of glasses is better than for the corresponding crystalline phases. It seems that the influence of the structural disorder

is so strong that the element-specific details of the interatomic potential are less important than in crystalline structures.

Complementing these steady-state computer experiments, simulations of shock waves and heat pulses in condensed matter were performed. Again one can clearly see the influence of structural order or disorder on the results and the outcome of the calculations.

In the crystalline structures it was possible to identify waves moving through the system. This is clearly connected to the relatively high stability of the modes contained in the induced wave packet. The behavior of the wave packet reflects the elastic properties of the solid, e.g., one can calculate the sound velocity, from which one can then deduce the corresponding elastic constant. In contrast glasses do not show clearly developed propagating waves after inducing a heat pulse or a shock wave into the structure. Again, the reason for this behavior can be found in the short lifetimes and mean free paths of the eigenmodes or phonons of glasses where the disorder plays the role of scatterers for the modes.

ACKNOWLEDGMENTS

We are indebted to V. I. Kozub and H. R. Schober for valuable discussions and critically reading the manuscript. We gratefully acknowledge funding by the Deutsche Forschungsgemeinschaft through the Sonderforschungsbereich 408. This work was conducted within the GMD research group "Computational Methods in Chemistry." Parts of the calculations are performed on the IBM SP2 computer at the Institute for Algorithms and Scientific Computing (SCAI), German National Research Center for Information Technology.

*Present address: Institut für Physikalische und Theoretische Chemie, Universität Bonn, Wegelerstr. 12, D-53115 Bonn, Germany.

- ¹R. C. Zeller and R. O. Pohl, *Phys. Rev. B* **4**, 2029 (1971).
- ²P. W. Anderson, B. I. Halperin, and C. M. Varma, *Philos. Mag.* **25**, 1 (1972).
- ³W. A. Phillips, *J. Low Temp. Phys.* **7**, 351 (1972).
- ⁴V. G. Karpov, M. I. Klinger, and F. N. Ignatiev, *Sov. Phys. JETP* **57**, 439 (1987).
- ⁵A. J. C. Ladd, B. Moran, and W. G. Hoover, *Phys. Rev. B* **34**, 5058 (1986).
- ⁶D. J. Evans, W. G. Hoover, B. H. Failor, B. Moran, and A. J. C. Ladd, *Phys. Rev. A* **28**, 1016 (1983).
- ⁷J. P. Hansen and M. L. Klein, *Phys. Rev. B* **13**, 878 (1976).
- ⁸D. H. Tsai and R. A. MacDonald, *Phys. Rev. B* **14**, 4714 (1976).
- ⁹D. H. Tsai and R. A. MacDonald, *J. Phys. C* **6**, L171 (1973).
- ¹⁰A. J. C. Ladd and W. G. Hoover, *Phys. Rev. B* **28**, 1756 (1983).
- ¹¹A. B. Belonoshko, *Science* **275**, 955 (1997).
- ¹²B. L. Holian and P. S. Lomdahl, *Science* **280**, 2085 (1998).
- ¹³P. B. Allen and J. L. Feldman, *Phys. Rev. B* **48**, 12 581 (1993).
- ¹⁴J. Michalski, *Phys. Rev. B* **45**, 7054 (1992).
- ¹⁵J. Donohue, *The Structures of the Elements* (Wiley, New York, 1974), p. 370.
- ¹⁶R. W. G. Wyckoff, *Crystal Structures* (Krieger, Malabar, FL, 1982), p. 36.
- ¹⁷C. Oligschleger, R. O. Jones, S. M. Reimann, and H. R. Schober, *Phys. Rev. B* **53**, 6165 (1996).
- ¹⁸D. Hohl and R. O. Jones, *Phys. Rev. B* **43**, 3856 (1991).

- ¹⁹V. E. Bondybey and J. H. English, *J. Chem. Phys.* **72**, 6479 (1980).
- ²⁰*Selected Values of the Thermodynamic Properties of the Elements*, edited by R. Hultgren, P. D. Desai, and D. T. Hawkins (American Society for Metals, Metals Park, OH, 1973).
- ²¹K. C. Mills, *Thermodynamic Data for Inorganic Sulphides, Selenides and Tellurides* (Butterworths, London, 1974).
- ²²R. W. G. Wyckoff, *Crystal Structures* (Ref. 16), p. 312.
- ²³C. A. Angell and W. Sichina, *Ann. (N.Y.) Acad. Sci.* **279**, 53 (1976).
- ²⁴A. C. Wright and R. N. Sinclair, *J. Non-Cryst. Solids* **76**, 351 (1985).
- ²⁵A. C. Wright, *J. Non-Cryst. Solids* **106**, 1 (1988).
- ²⁶P. Vashishta, R. K. Kalia, J. P. Rino, and I. Ebbsjö, *Phys. Rev. B* **41**, 12 197 (1990).
- ²⁷*Selen, Gmelin Handbuch der Anorganischen Chemie*, 8th ed., Ergänzungsband A3, edited by G. Czack, G. Kirschstein, and H. K. Kugler (Springer, Berlin Heidelberg, 1981), and references therein.
- ²⁸C. Oligschleger and H. R. Schober, *Physica A* **201**, 391 (1993).
- ²⁹C. Oligschleger (unpublished).
- ³⁰*Simulations of Liquids and Solids*, edited by G. Cicotti, D. Frenkel, and I. R. McDonald (North Holland, Amsterdam, 1987).
- ³¹M. P. Allen and D. J. Tildesley, *Computer Simulation of Liquids* (Clarendon, Oxford, 1987).
- ³²J. P. Hansen and I. R. McDonald, *Theory of Simple Liquids* (Academic, New York, 1976).

- ³³D.W. Heermann, *Computer Simulation Methods* (Springer, Berlin, 1990).
- ³⁴S. Nosé and M. L. Klein, *Mol. Phys.* **50**, 1055 (1983).
- ³⁵J. H. Dickey and A. Paskin, *Phys. Rev.* **128**, 2589 (1969).
- ³⁶D. Beeman and R. Alben, *Adv. Phys.* **26**, 339 (1977).
- ³⁷H. Ibach and H. Lüth, *Festkörperphysik* (Springer, Berlin, 1981).
- ³⁸R. A. MacDonald and D. H. Tsai, *Phys. Rep.* **46**, 1 (1978).
- ³⁹R. D. Mountain and R. A. MacDonald, *Phys. Rev. B* **28**, 3022 (1983).
- ⁴⁰H. B. G. Casimir, *Physica* (Amsterdam) **5**, 595 (1938).
- ⁴¹N. W. Ashcroft and N. D. Mermin, *Solid State Physics* (HRW, Saunders, 1987).
- ⁴²H. R. Schober and W. Petry, in *Material Science and Technology*, edited by R. W. Cahn, P. Haasen, and E. J. Kramer (VCH, Weinheim, 1991), Vol. 1.
- ⁴³B. T. Smith, J. M. Boyle, J. J. Dongarra, B. S. Garbow, Y. Ikebe, V. C. Klema, and C. B. Moler, *Matrix Eigensystem Routines—EISPACK Guide* (Springer-Verlag, Berlin, 1976).
- ⁴⁴H. R. Glyde, J. P. Hansen, and M. L. Klein, *Phys. Rev. B* **16**, 3476 (1977).
- ⁴⁵C.-Y. Ho and R. W. Powell (unpublished).
- ⁴⁶M. Meißner and D. Wobig, in *Physics of Selenium and Tellurium*, edited by E. Gerlach and P. Grosse (Springer, Berlin, 1979).
- ⁴⁷D. G. Cahill and R. O. Pohl, *Phys. Rev. B* **35**, 4067 (1987).
- ⁴⁸C. Oligschleger (unpublished).
- ⁴⁹C. Oligschleger and J. C. Schön, *J. Phys.: Condens. Matter* **9**, 1049 (1997).
- ⁵⁰C. Oligschleger (unpublished).
- ⁵¹H. R. Schober and C. Oligschleger, *Phys. Rev. B* **53**, 11 469 (1996).